

Supplementary Materials for

Persistence and decay of human antibody responses to the receptor binding domain of SARS-CoV-2 spike protein in COVID-19 patients

Anita S. Iyer, Forrest K. Jones, Ariana Nodoushani, Meagan Kelly, Margaret Becker, Damien Slater, Rachel Mills, Erica Teng, Mohammad Kamruzzaman, Wilfredo F. Garcia-Beltran, Michael Astudillo, Diane Yang, Tyler E. Miller, Elizabeth Oliver, Stephanie Fischinger, Caroline Atyeo, A. John Iafate, Stephen B. Calderwood, Stephen A. Lauer^c, Jingyou Yu, Zhenfeng Li, Jared Feldman, Blake M. Hauser, Timothy M. Caradonna, John A. Branda, Sarah E. Turbett, Regina C. LaRocque, Guillaume Mellon, Dan H. Barouch, Aaron G. Schmidt, Andrew S. Azman, Galit Alter, Edward T Ryan, Jason B. Harris, Richelle C. Charles*

*Corresponding author. Email: rcharles@mgh.harvard.edu

Published First Release 8 October 2020, *Sci. Immunol.*

DOI: 10.1126/sciimmunol.abe0367

This PDF file includes:

Figure S1: Number of PCR positive cases with a sample taken during each week since symptom onset.

Figure S2. Smooth average measurements of IgG, IgM, and IgA against SARS-CoV-2 spike protein receptor binding domain among PCR positive cases across time.

Figure S3. Individual trajectories for 16 randomly selected individuals with 4 or more measurements.

Figure S4. Measurements of IgG, IgM, and IgA against SARS-CoV-2 spike protein receptor binding domain among pre-pandemic controls and symptomatic PCR positive cases.

Figure S5. Receiver operating characteristic curve from random forest models and isotype contributions.

Figure S6. Confusion matrices and out-of-bag error estimates for random forest models.

Figure S7. Confusion matrices and out-of-bag error estimates for random forest models with downsampled controls.

Figure S8. Measurements of IgG, IgA, and IgM against the RBD of other coronaviruses among pre-pandemic controls and PCR positive cases.

Figure S9. Correlation between plasma and dried blood spot measurements (DBS).

Table S1. Full amino acid sequences of the coronavirus receptor-binding domains (RBDs) used in this study.

Table S2. Predictive accuracy of multiple isotypes for classifying controls and cases over time since symptom onset.

Table S3. Parametric estimates of median time to seroconversion for each isotype by different patient characteristics.

Other Supplementary Material for this manuscript includes the following:

(available at immunology.sciencemag.org/cgi/content/full/5/52/eabe0367/DC1)

Table S4. Raw data file (Excel spreadsheet).

Persistence and decay of human antibody responses to the receptor binding domain of SARS-CoV-2 spike protein in COVID-19 patients

Anita S. Iyer^{a,b*}, Forrest K. Jones^{c*}, Ariana Nodoushani^{a*}, Meagan Kelly^a, Margaret Becker^a, Damien Slater^a, Rachel Mills^a, Erica Teng^a, Mohammad Kamruzzaman^a, Wilfredo F. Garcia-Beltran^d, Michael Astudillo^d, Diane Yang^d, Tyler E. Miller^d, Elizabeth Oliver^a, Stephanie Fischinger^e, Caroline Atyeo^e, A. John Iafrate^d, Stephen B. Calderwood^{a,b,f}, Stephen A. Lauer^c, Jingyou Yu^g, Zhenfeng Li^g, Jared Feldman^e, Blake M. Hauser^e, Timothy M. Caradonna^e, John A. Branda^d, Sarah E. Turbett^{a,b,d}, Regina C. LaRocque^{a,b}, Guillaume Mellon^a, Dan H. Barouch^{e,g}, Aaron G. Schmidt^{e,f}, Andrew S. Azman^c, Galit Alter^e, Edward T Ryan^{a,b,h}, Jason B. Harris^{a,i#}, Richelle C. Charles^{a,b##}

Supplementary Materials

Figure S1: Number of PCR positive cases with a sample taken during each week since symptom onset.

Figure S2. Smooth average measurements of IgG, IgM, and IgA against SARS-CoV-2 spike protein receptor binding domain among PCR positive cases across time.

Figure S3. Individual trajectories for 16 randomly selected individuals with 4 or more measurements.

Figure S4. Measurements of IgG, IgM, and IgA against SARS-CoV-2 spike protein receptor binding domain among pre-pandemic controls and symptomatic PCR positive cases.

Figure S5. Receiver operating characteristic curve from random forest models and isotype contributions.

Figure S6. Confusion matrices and out-of-bag error estimates for random forest models.

Figure S7. Confusion matrices and out-of-bag error estimates for random forest models with downsampled controls.

Figure S8. Measurements of IgG, IgA, and IgM against the RBD of other coronaviruses among pre-pandemic controls and PCR positive cases.

Figure S9. Correlation between plasma and dried blood spot measurements (DBS).

Table S1. Full amino acid sequences of the coronavirus receptor-binding domains (RBDs) used in this study.

Table S2. Predictive accuracy of multiple isotypes for classifying controls and cases over time since symptom onset.

Table S3. Parametric estimates of median time to seroconversion for each isotype by different patient characteristics.

Table S4. Raw data file (Excel spreadsheet).

Figure S1. Number of PCR positive cases with a sample taken during each week since symptom onset. The date of symptom onset could not be determined for three individuals and the severity index was missing for one individual.

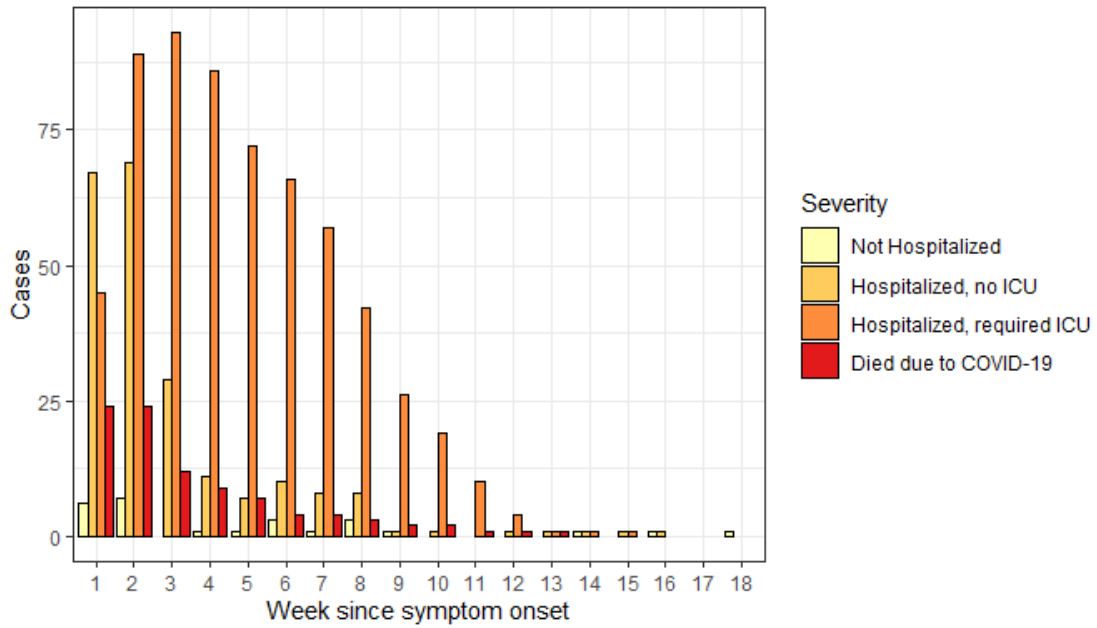


Figure S2. Smooth average measurements of IgG, IgM, and IgA against SARS-CoV-2 spike protein receptor binding domain among PCR positive cases across time. Limit of detection was artificially set at 0.3 $\mu\text{g/mL}$ for IgM and IgG to match that of IgA. Points were jittered horizontally. A) All cases are shown. Cases are categorized by B) clinical severity and C) immunosuppression status.

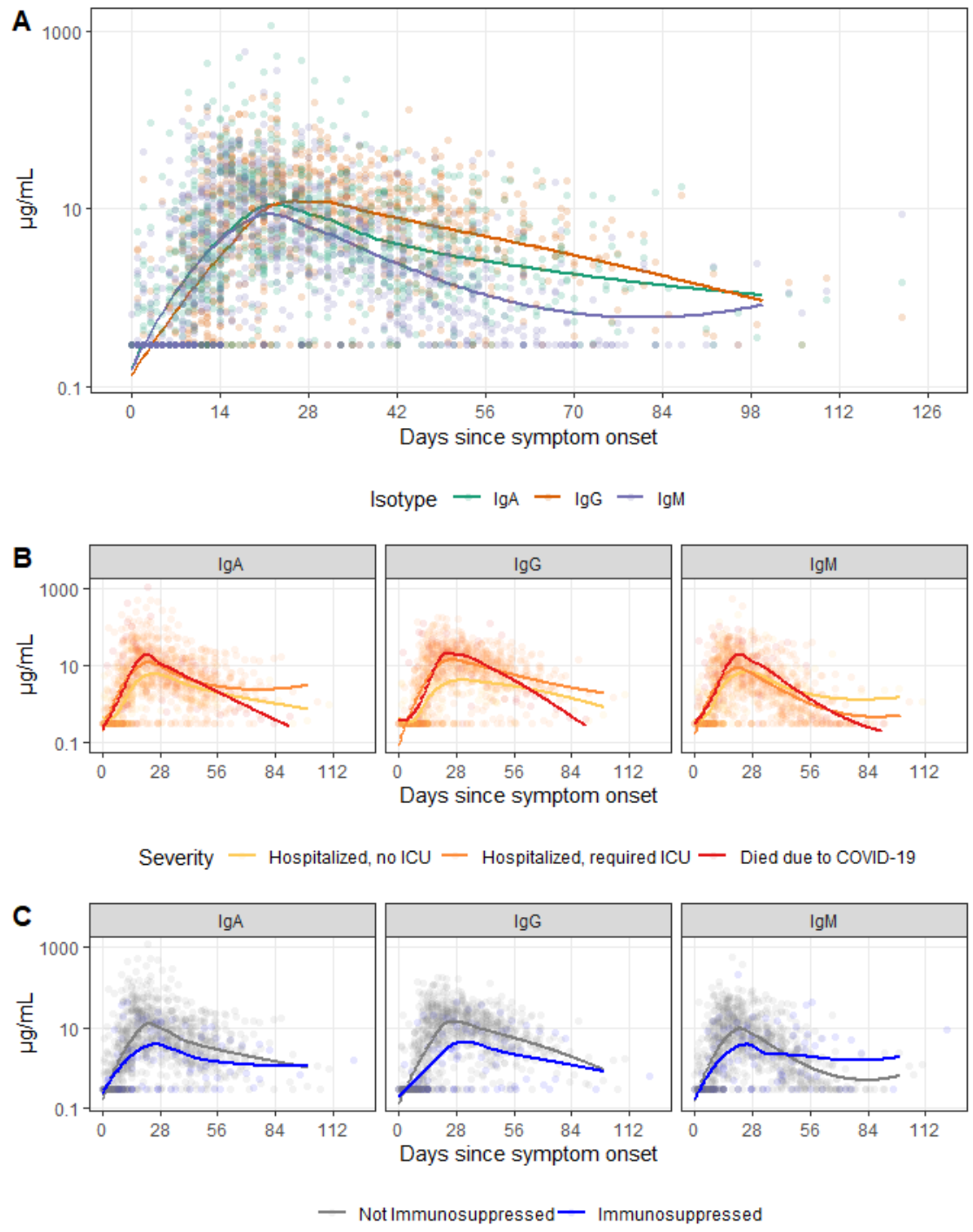


Figure S3. Individual trajectories for 16 randomly selected individuals with 4 or more measurements. Patient ID numbers are shown in gray boxes.

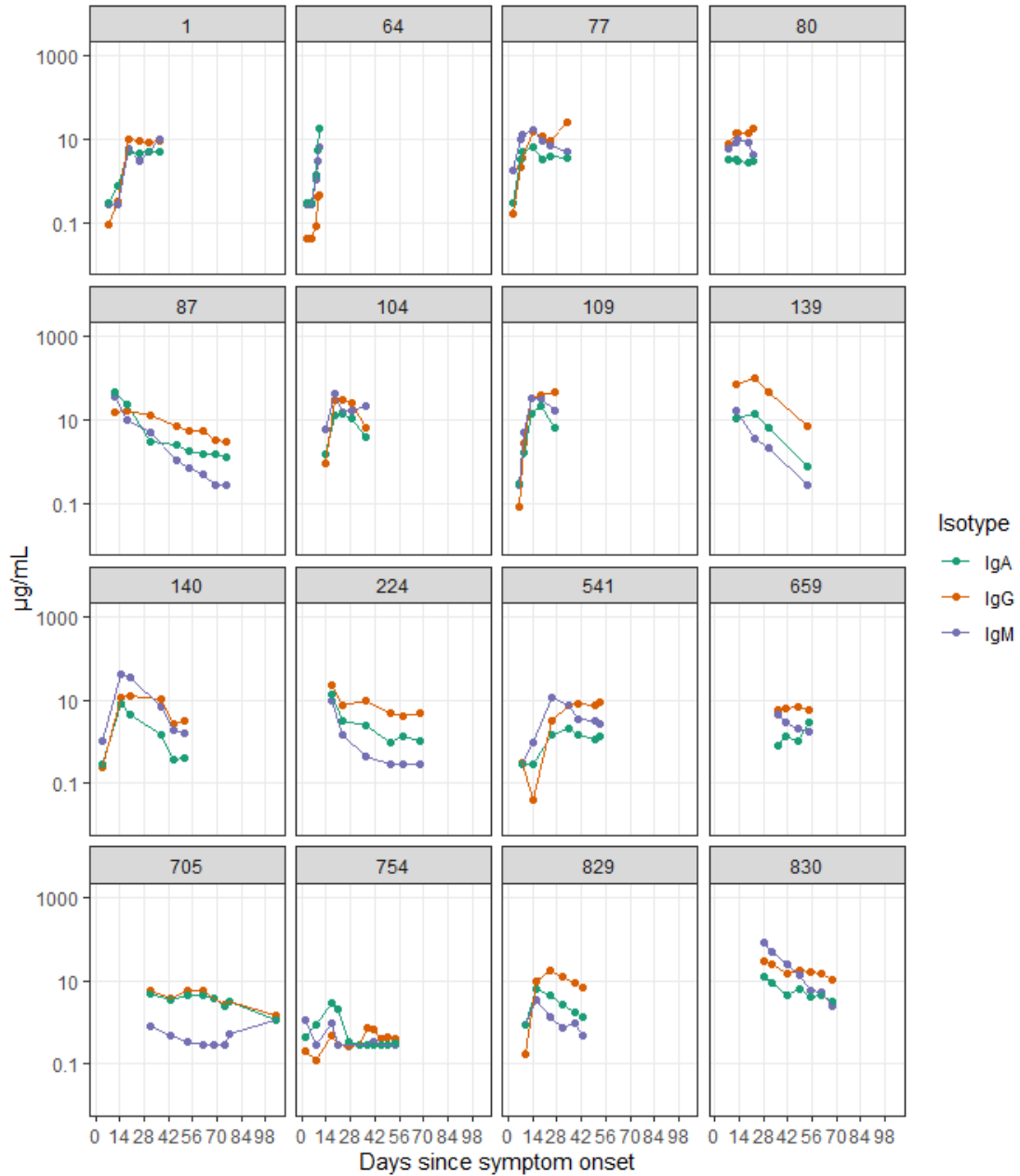


Figure S4. Measurements of IgG, IgM, and IgA against SARS-CoV-2 spike protein receptor binding domain among pre-pandemic controls and symptomatic PCR positive cases. Black dashed line is at $0.57 \mu\text{g/mL}$ for IgG, $2.63 \mu\text{g/mL}$ for IgM, and $2.02 \mu\text{g/mL}$ for IgA.

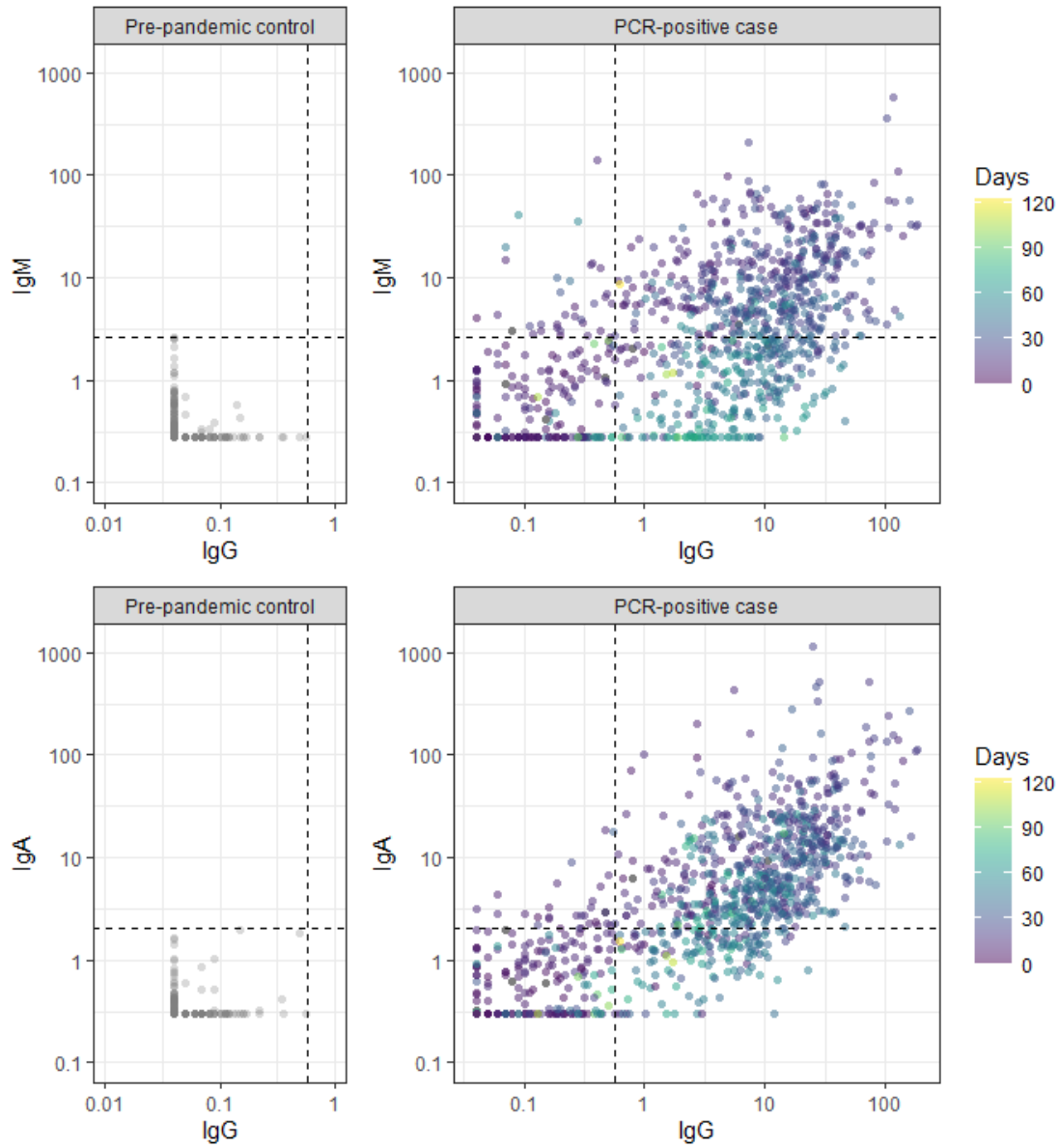


Figure S5. Receiver operating characteristic curve from random forest models and isotype contributions. Each panel shows the ROC curves for cross-validated random forest models fit to serological measurements taken (A) under 7 days (cvAUC: 0.64), (B) 8-14 days (cvAUC: 0.92), (C) 15-28 days (cvAUC: 1.00) and over 28 days (cvAUC: 1.00) after symptom onset of PCR positive cases and pre-pandemic controls. Each blue line is one of ten cross-validated ROC curves for a specific time point. Median relative importance of each serological marker is shown in each bar graph.

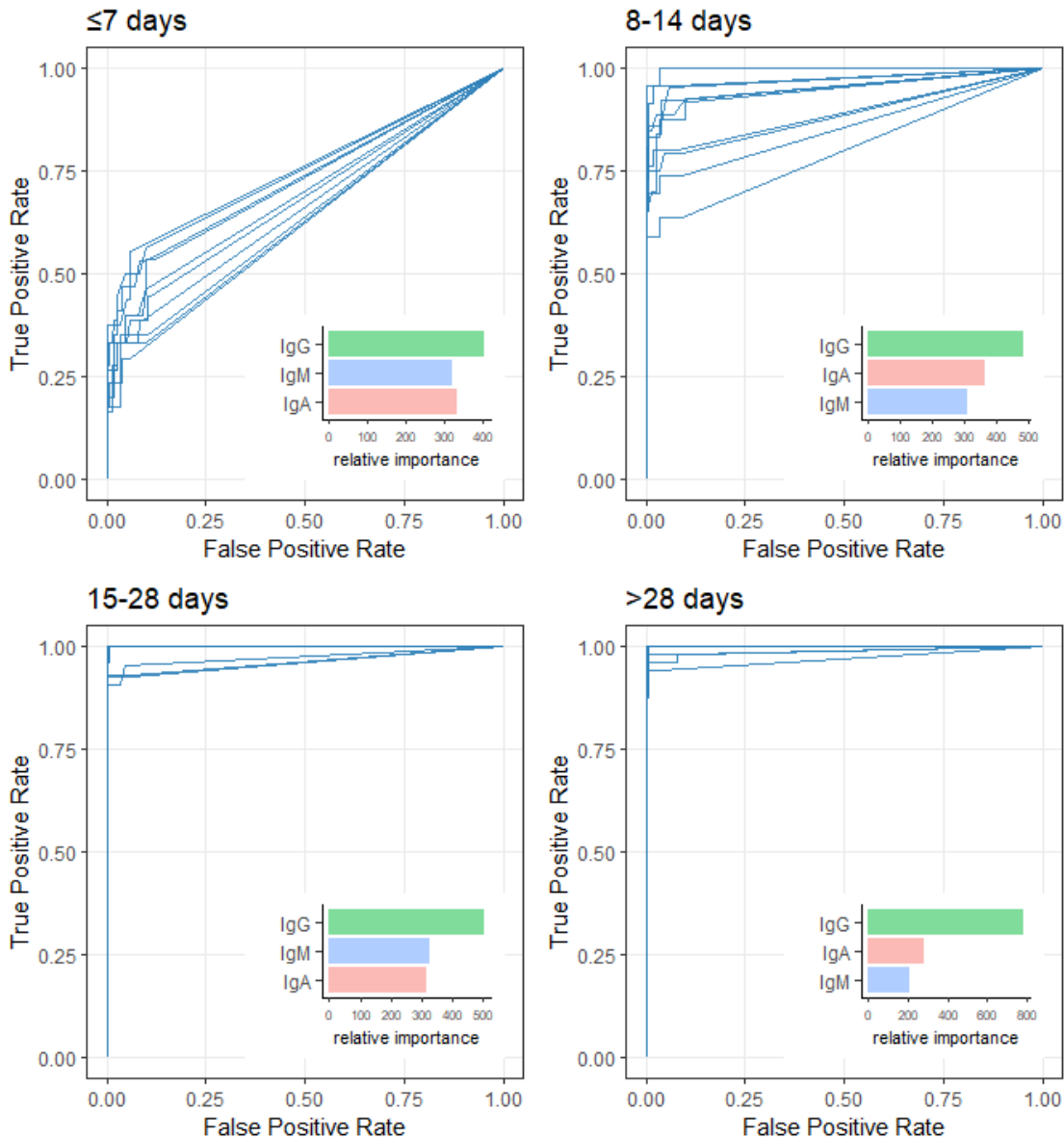


Figure S6. Confusion matrices and out-of-bag error estimates for random forest models.

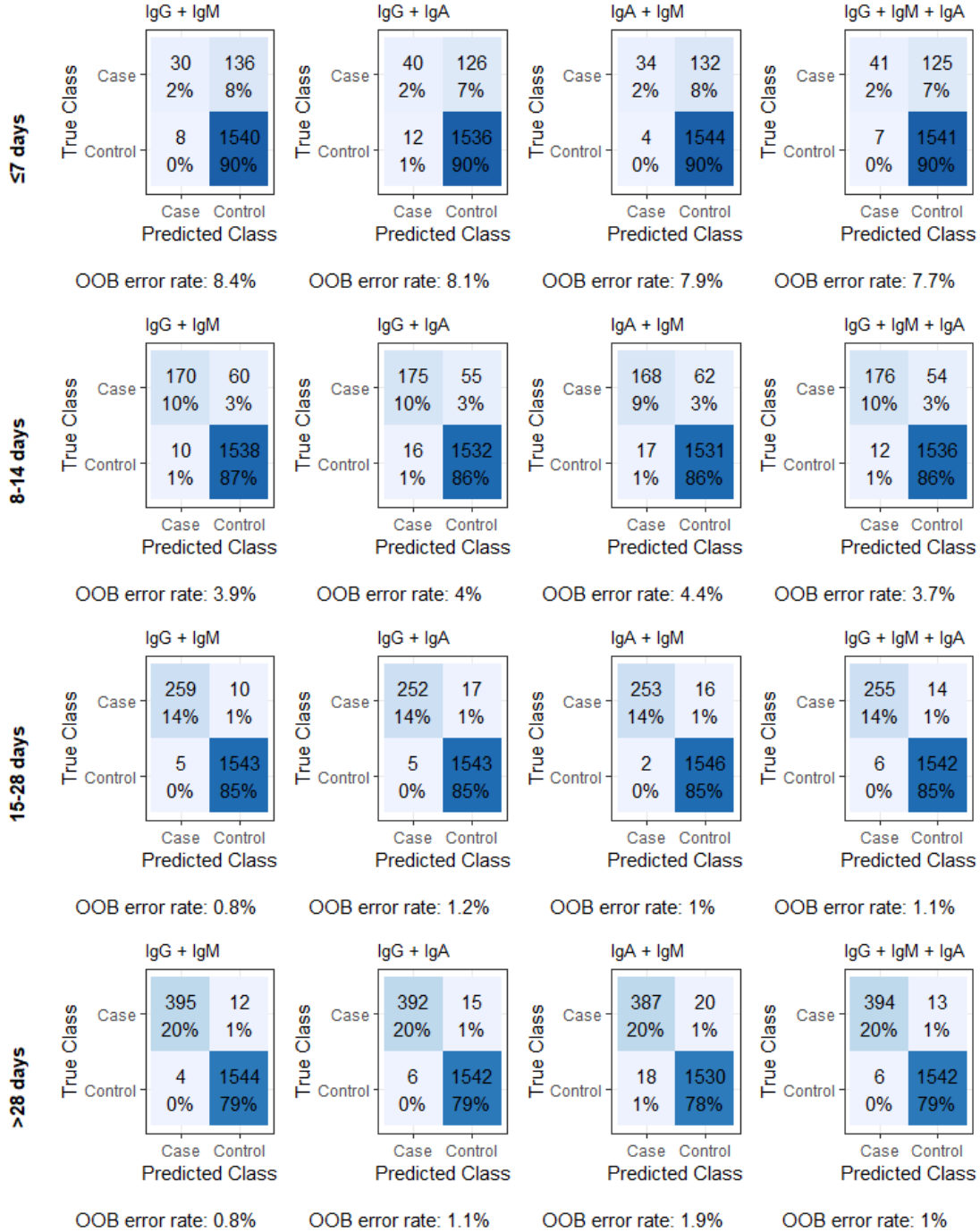


Figure S7. Confusion matrices and out-of-bag error estimates for random forest models with downsampled controls. Controls were downsampled to have the same number of samples as cases for a given period.

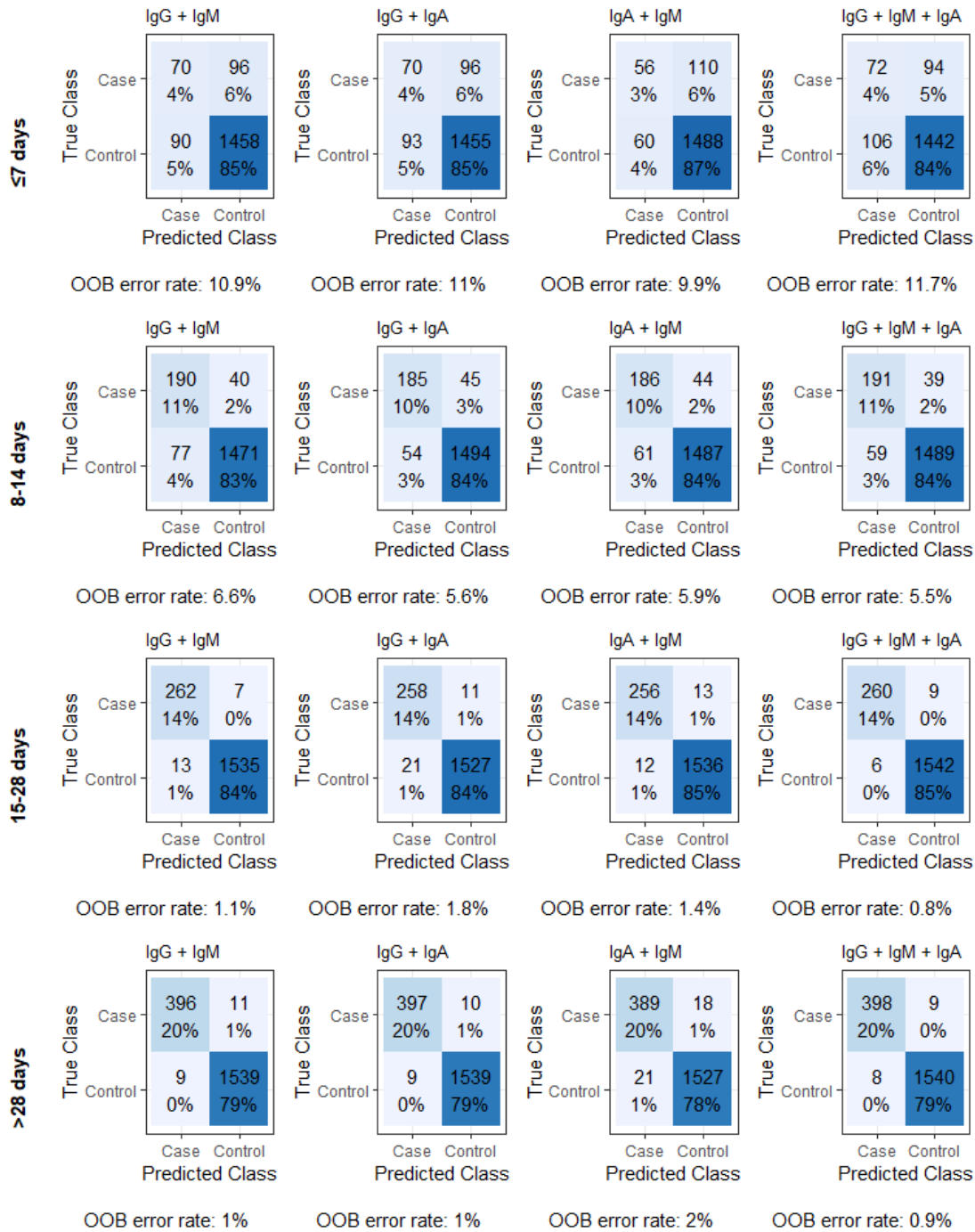


Figure S8. Measurements of IgG, IgA, and IgM against the RBD of other coronaviruses among pre-pandemic controls and PCR positive cases. Each dot represents a unique measurement of a serological marker (Row A: IgG, Row B: IgA, Row C: IgM) in pre-pandemic controls (left panels) and PCR positive cases (right panels) for each coronavirus. Each line connects measurements (dots) for individuals.

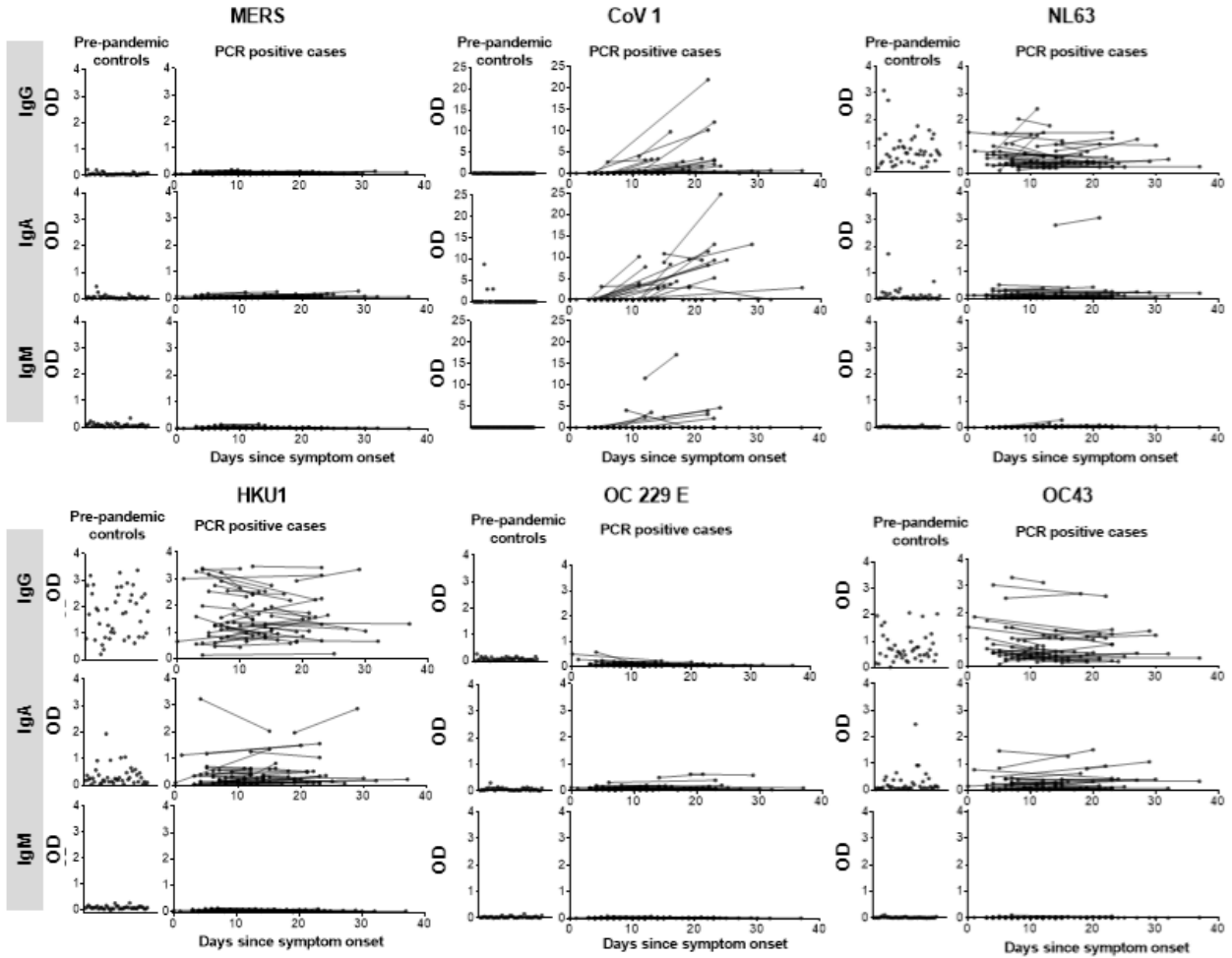


Figure S9. Correlation between plasma and dried blood spot measurements (DBS). Plot of anti-RBD antibody IgG measurement in plasma versus DBS of 20 COVID cases (at 2 timepoints) and 20 pre-pandemic controls. The Pearson correlation coefficient (r) is shown. The dotted gray lines represent the concentration cut-off for seropositivity with plasma.

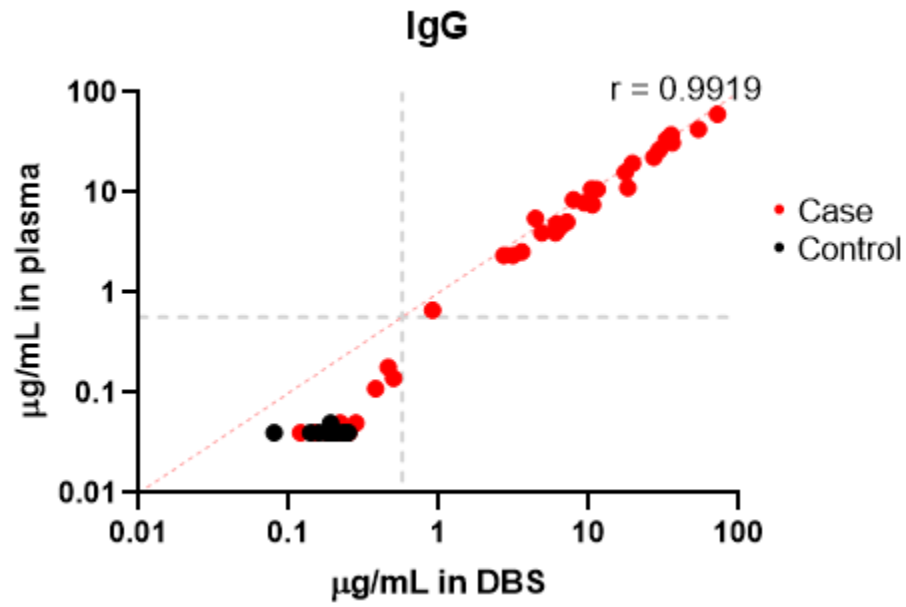


Table S1. Full amino acid sequences of the coronavirus receptor-binding domains (RBDs) used in this study. In parentheses are the GenBank accession numbers from which the RBDs derive. Underlined is the HRV-3C protease site, the 8xHis and streptavidin-binding peptide (SBP) purification tags.

Coronavirus	RBD Sequence
SARS-CoV-2	>SARS2_RBD (MN975262) RVQPTE ^S IVRFPNITNLC ^P FG ^E VF ^N AT ^R FA ^S VY ^A W ^N R ^K RI ^S NC ^V AD ^Y SV ^L Y ^N S ^A S ^F ST ^F K ^C Y ^G V ^S PT ^K LN DL ^C F ^T N ^V Y ^A D ^S F ^V IR ^G DE ^V R ^Q I ^A P ^G Q ^T G ^K I ^A D ^Y N ^Y K ^L P ^D D ^F T ^G C ^V I ^A W ^N S ^N N ^L D ^S K ^V G ^G N ^Y N ^Y L ^R L ^F R ^K SN ^L K ^P F ^E R ^D I ^S T ^E I ^Y Q ^A G ^S T ^P C ^N G ^V E ^G F ^N C ^Y F ^L Q ^S Y ^G F ^Q P ^T N ^G V ^G Y ^Q P ^Y R ^V V ^V L ^S F ^E L ^L H ^A P ^A T ^V C ^G P ^K K ^G A ^G S ^S L ^E V ^L F ^Q G ^P G ^S G ^S S ^H H ^H H ^H H ^H H ^H G ^G S ^G S ^S M ^D E ^K T ^T G ^W R ^G G ^H V ^V E ^G L ^A G ^E L ^E Q ^L R ^A R ^L E ^H H ^P Q ^G Q ^R E ^P
SARS-CoV-1	>SARS1_RBD (AAP13441.1) RVVPSGDVVRFPNITNLC ^P FG ^E VF ^N AT ^K F ^P S ^V Y ^A W ^E R ^K K ^I S ^N C ^V AD ^Y SV ^L Y ^N S ^T F ^F ST ^F K ^C Y ^G V ^S AT ^K LN DL ^C F ^S N ^V Y ^A D ^S F ^V V ^K G ^D D ^V R ^Q I ^A P ^G Q ^T G ^V I ^A D ^Y N ^Y K ^L P ^D D ^F M ^G C ^V L ^A W ^N T ^R N ^I D ^A T ^S T ^G N ^Y N ^Y K ^Y R ^L R ^H G ^K L ^R P ^F E ^R D ^I S ^N V ^P F ^S P ^D G ^K P ^C T ^P P ^A L ^N C ^Y W ^L N ^D Y ^G F ^Y T ^T T ^G I ^G Y ^Q P ^Y R ^V V ^V L ^S F ^E L ^L N ^A P ^A T ^V C ^G P ^K L G ^A G ^S S ^L E ^V L ^F Q ^G P ^G S ^G S ^S H ^H H ^H H ^H H ^H G ^G S ^G S ^S M ^D E ^K T ^T G ^W R ^G G ^H V ^V E ^G L ^A G ^E L ^E Q ^L R ^A R ^L E ^H H ^P Q ^G Q ^R E ^P
MERS	>MERS_RBD (AFY13307.1) EAKPSGSVVEQAEGVECDFSP ^L LSG ^T PP ^Q VY ^N F ^K R ^L V ^F T ^N C ^N Y ^N L ^T K ^L L ^S L ^F S ^V N ^D F ^T C ^S Q ^I S ^P A ^I A ^S N CY ^S S ^L I ^L D ^Y F ^S Y ^P L ^S M ^K S ^D L ^S V ^S S ^A G ^P I ^S Q ^F N ^Y K ^Q S ^F S ^N P ^T C ^L I ^L A ^T V ^P H ^N L ^T T ^I T ^K P ^L K ^Y S ^Y I ^N K ^C S ^R F L ^S D ^D R ^T E ^V P ^Q L ^V N ^A N ^Q Y ^S P ^C V ^S I ^V P ^S T ^V W ^E D ^G D ^Y R ^K Q ^L S ^P L ^E G ^G W ^L V ^A S ^G S ^T V ^A M ^T E ^Q L ^Q M ^G F ^G I ^T V ^Q Y ^G T ^D T ^N S ^V C ^P K ^L E ^F A ^N D ^T K ^I A ^S Q ^L G ^A G ^S S ^L E ^V L ^F Q ^G P ^G S ^G S ^S H ^H H ^H H ^H H ^H G ^G S ^G S ^S M ^D E ^K T ^T G ^W R ^G G ^H V ^V E ^G L ^A G ^E L ^E Q ^L R ^A R ^L E ^H H ^P Q ^G Q ^R E ^P
HKU1	>HKU1_RBD (AAT98580.1) TVKPVATVHRRIPDL ^P DC ^D ID ^K W ^L N ^N F ^N V ^P S ^P L ^N W ^E R ^K I ^F S ^N C ^N F ^N L ^S T ^L L ^R L ^V H ^T D ^S F ^S C ^N N ^F D ^E S ^K I ^Y G ^S C ^F K ^S I ^V L ^D K ^F A ^I P ^N S ^R R ^S D ^L Q ^L G ^S S ^G F ^L Q ^S S ^N Y ^I D ^T T ^S S ^S C ^Q L ^Y S ^L P ^A I ^N V ^T I ^N N ^Y N ^P S ^S W ^N R ^R Y ^G F ^N N ^F N ^L S ^S H ^S V ^V Y ^S R ^Y C ^F S ^V N ^N T ^F C ^P C ^A K ^P S ^F A ^S S ^C K ^S H ^K P ^P S ^A S ^C P ^I G ^T N ^Y R ^S C ^E S ^T T ^V L ^D H ^T D ^W C ^R C ^S C ^L P ^D P ^I T ^A Y ^D P ^R S ^C S ^Q K ^K S ^L V ^G V ^G E ^H C ^A G ^F V ^D E ^E K ^C G ^V L ^D G ^S Y ^N V ^S C ^L C ^S T ^D A ^F L ^G W ^S Y ^D T ^C V ^S N ^N R ^C N I ^F S ^N F ^I L ^N G ^I N ^S G ^T T ^C S ^N D ^L L ^Q P ^N T ^E V ^F T ^D V ^C V ^D Y ^D L ^Y G ^I T ^G Q ^G I ^F K ^E V ^S A ^V Y ^Y N ^S W ^Q N ^L L ^Y D ^S N ^G N ^I I ^G F ^K D ^F V ^T N ^K T ^Y N ^I F ^P C ^Y A ^G G ^A G ^S S ^L E ^V L ^F Q ^G P ^G S ^G S ^S H ^H H ^H H ^H H ^H G ^G S ^G S ^S M ^D E ^K T ^T G ^W R ^G G ^H V ^V E ^G L ^A G ^E L ^E Q ^L R ^A R ^L E ^H H ^P Q ^G Q ^R E ^P
OC229E	>OC229E_RBD (AAK32191) VSLPVYHKHMFIVLYVDFK ^P Q ^S G ^G G ^K C ^F N ^C Y ^P A ^G V ^N I ^T L ^A N ^F N ^E T ^K G ^P L ^C V ^D T ^S H ^F T ^T K ^Y V ^A V ^Y A ^N V ^G R ^W S ^A S ^I N ^T G ^N C ^P F ^S F ^G K ^V N ^N F ^V K ^F G ^S V ^C F ^S L ^K D ^I P ^G G ^C A ^M P ^I V ^A N ^W A ^Y S ^K Y ^Y T ^I G ^T L ^V S ^W S ^D G ^D G ^I T ^G V ^P Q P ^V E ^G V ^G A ^G S ^S L ^E V ^L F ^Q G ^P G ^S G ^S S ^H H ^H H ^H H ^H H ^H G ^G S ^G S ^S M ^D E ^K T ^T G ^W R ^G G ^H V ^V E ^G L ^A G ^E L ^E Q ^L R ^A R ^L E ^H H ^P Q ^G Q ^R E ^P
OC43	>OC43_RBD (AAT84362) RRKPNLPNCNIEAWLNDKSVPSPLNWERK ^T F ^S N ^C N ^F N ^M S ^S L ^M S ^F I ^Q A ^D S ^F T ^C N ^N I ^D A ^A K ^I Y ^G M ^C F ^S S ^I T ^I D ^K F ^A I ^P N ^G R ^K V ^D L ^Q L ^G N ^L G ^Y L ^Q S ^F N ^Y R ^I D ^T T ^A T ^S C ^Q L ^Y N ^L P ^A A ^N V ^S V ^S R ^F N ^P S ^T W ^N K ^R F ^G F ^I E ^D S ^V F ^K P R ^P A ^G V ^L T ^N H ^D V ^V Y ^A Q ^H C ^F K ^A P ^K N ^F C ^P C ^K L ^N G ^S C ^V G ^S G ^P G ^K N ^N G ^I G ^T C ^P A ^G T ^N Y ^L T ^C D ^N L ^C T ^P D ^P I ^T F ^T G ^T Y ^K C ^P Q ^T K ^S L ^V G ^I G ^E H ^C S ^G L ^A V ^K S ^D Y ^C G ^G N ^S C ^T C ^R P ^Q A ^F L ^G W ^S A ^D S ^C L ^Q G ^D K ^C N ^I F ^A N ^F I ^L H ^D V ^N S ^G L ^T C ^S T ^D L ^Q K ^A N ^T G ^A G ^S S ^L E ^V L ^F Q ^G P ^G S ^G S ^S H ^H H ^H H ^H H ^H G ^G S ^G S ^S M ^D E ^K T ^T G ^W R ^G G ^H V ^V E ^G L ^A G ^E L ^E Q ^L R ^A R ^L E ^H H ^P Q ^G Q ^R E ^P
NL63	>NL63_RBD (AKT07952) QHTDIN ^F T ^A T ^A S ^F G ^G S ^C Y ^V C ^K P ^H Q ^V N ^I S ^L N ^G N ^T S ^V C ^V R ^T S ^H F ^S I ^R Y ^I Y ^N R ^V K ^S G ^S P ^D S ^S W ^H I ^Y L ^K S ^G T ^C P ^F S ^F S ^K L ^N N ^F Q ^K F ^K T ^I C ^F S ^T V ^E V ^P G ^S C ^N F ^L E ^A T ^W H ^Y T ^S Y ^T I ^V G ^A L ^Y V ^T W ^S E ^G N ^S I ^T G ^V P ^Y P ^V S ^G I G ^A G ^S S ^L E ^V L ^F Q ^G P ^G S ^G S ^S H ^H H ^H H ^H H ^H G ^G S ^G S ^S M ^D E ^K T ^T G ^W R ^G G ^H V ^V E ^G L ^A G ^E L ^E Q ^L R ^A R ^L E ^H H ^P Q ^G Q ^R E ^P

Table S2. Predictive accuracy of multiple isotypes for classifying controls and cases over time since symptom onset. Random forest models were used to calculate cvAUC. The isotype cut-offs chosen for calculating sensitivity were the maximum concentration ($\mu\text{g/mL}$) found among pre-pandemic controls (IgG: 0.57, IgM: 2.63, IgA: 2.02). Samples with measurements above at least one cut-off were classified as cases.

Isotypes	Days since symptom onset	cvAUC (95% CI)	Sensitivity (95% CI)
IgA + IgG	≤ 7 days	0.68 (0.59–0.78)	0.10 (0.06–0.15)
	8-14 days	0.91 (0.87–0.96)	0.58 (0.51–0.66)
	15-28 days	0.99 (0.96–1.00)	0.96 (0.93–0.99)
	> 28 days	0.99 (0.97–1.00)	0.95 (0.91–0.98)
IgM + IgG	≤ 7 days	0.68 (0.59–0.77)	0.09 (0.04–0.14)
	8-14 days	0.92 (0.87–0.96)	0.59 (0.51–0.66)
	15-28 days	0.99 (0.97–1.00)	0.96 (0.93–0.99)
	> 28 days	0.99 (0.98–1.00)	0.96 (0.92–0.99)
IgM + IgA	≤ 7 days	0.65 (0.56–0.75)	0.09 (0.05–0.15)
	8-14 days	0.90 (0.85–0.95)	0.59 (0.52–0.66)
	15-28 days	0.98 (0.95–1.00)	0.95 (0.92–0.98)
	> 28 days	0.98 (0.95–1.00)	0.74 (0.66–0.81)
IgM + IgA + IgG	≤ 7 days	0.69 (0.60–0.78)	0.11 (0.06–0.16)
	8-14 days	0.92 (0.88–0.97)	0.63 (0.56–0.69)
	15-28 days	0.99 (0.97–1.00)	0.97 (0.95–0.99)
	> 28 days	0.99 (0.98–1.00)	0.96 (0.92–0.99)

Table S3. Parametric estimates of median time to seroconversion for each isotype by different patient characteristics. The isotype cutoffs chosen for seroconversion were the maximum concentration ($\mu\text{g/mL}$) found among pre-pandemic controls (IgG: 0.57, IgM: 2.63, IgA: 2.02). All models assumed that time to event followed a Weibull distribution. Bootstrap 95% confidence intervals are shown in parentheses. Not Hospitalized and Hospitalized, no ICU groups were combined due to small sample size.

Isotype	Characteristic	50th percentile (95% CI)	Difference (95% CI)
IgA	Age		
	<65 years	11.8 (10.5 – 13.1)	
	≥ 65 years	13.7 (10.6 – 17.5)	1.9 (-0.9 – 5.4)
	Sex		
	Male	11.8 (10.5 – 13.3)	
	Female	16.4 (12.4 – 21.8)	4.6 (1.1 – 9.3)
	Severity		
	Not Hospitalized / Hospitalized, no ICU	12.2 (10.9 – 13.6)	
	Hospitalized, required ICU	7.3 (5.5 – 9.5)	-4.9 (-6.9 – -2.8)
Died due to COVID-19	9.0 (6.2 – 12.2)	-3.2 (-6.1 – 0.2)	
IgG	Age		
	<65 years	10.7 (9.6 – 11.9)	
	≥ 65 years	13.3 (10.4 – 16.8)	2.6 (-0.0 – 5.9)
	Sex		
	Male	10.7 (9.7 – 11.8)	
	Female	14.2 (11.0 – 18.2)	3.5 (0.7 – 7.1)
	Severity		
	Not Hospitalized / Hospitalized, no ICU	10.9 (9.6 – 12.2)	
	Hospitalized, required ICU	6.9 (5.2 – 8.7)	-4.0 (-5.7 – -2.2)
Died due to COVID-19	10.1 (6.8 – 14.2)	-0.8 (-4.1 – 3.1)	
IgM	Age		
	<65 years	12.0 (10.7 – 13.6)	
	≥ 65 years	13.8 (9.9 – 18.8)	1.8 (-1.5 – 6.2)
	Sex		
	Male	12.1 (10.7 – 13.7)	
	Female	17.8 (12.9 – 23.7)	5.7 (1.4 – 11.0)
	Severity		
	Not Hospitalized / Hospitalized, no ICU	12.3 (10.7 – 14.2)	
	Hospitalized, required ICU	7.9 (5.8 – 10.2)	-4.4 (-6.9 – -2.0)
Died due to COVID-19	7.3 (4.9 – 10.8)	-5.0 (-7.8 – -1.4)	